TECHNISCHE MECHANIK
an open access journal

journal homepage: www.ovgu.de/techmech

Tech. Mech., Vol. 41, Is. 1, (2021), 24–33

Received: 14.04.2021
Accepted: 05.07.2021
Available online: 07.09.2021

Hashin-Shtrikman Bounds of Cubic Crystalline Aggregate Elasticity for poly-Si Solar Cells

Marcus Aßmus*, Rainer Glüge, Holm Altenbach,

Otto von Guericke University, Institute of Mechanics, Universitätsplatz 2, 39108 Magdeburg, Germany

Dedicated to Prof. Henryk Petryk on the occasion of his 70th birthday

Abstract: In present work, the studies on the analytical determination of polycrystalline silicon effective mechanical properties for solar cells based on a class of bounds are intensified while second-order estimates are introduced. Thereby the fundamental aspects of the Hashin-Shtrikman bounds of linear elastic properties for a cubic crystal aggregate are surveyed. The aggregate is considered homogeneous and isotropic in a statistical sense. This framework is exploited to determine improved bounds in comparison to the classically applied first-order bounds. The results gained are related to previously published Voigt and Reuss bounds and to experimental data. Improvements and problems are highlighted and discussed.

Keywords: solar energy materials, solar cells, cubic crystalline aggregates, homogenization, linear elastic properties

1 Introduction

1.1 Motivation

Polycrystalline silicon (poly-Si) solar cells are crystalline aggregates built from silicon monocrystals obeying cubic symmetry. As usual, the concept of effective properties is applied since the characteristic size of the component under consideration is considerably larger than the characteristic length of its microstructure. This is true for poly-Si solar cells, cf. Aßmus et al. (2020). To determine effective properties, numerous procedures are available which are summarized in some comprehensive treatises, e.g., Milton (2002), Nemat-Nasser and Hori (1993), or Dvorak (2013). It is well known that the exploitation of analytical methods is much less time-consuming than applying computational approaches such as the finite element method and others. We therefore prefer analytical approaches for the present investigations. In Aßmus et al. (2020), for present material, first-order bounds based on Voigt (1910) and Reuss (1929) are determined, and an approximation based on Hill (1952) is introduced for comparison to experimental data. Thereby a polycrystalline aggregate with irregular shaped and randomly oriented crystals is anticipated, which is statistically isotropic due to a sufficiently large number of crystals obeying cubic symmetry. Commonly, the range of the elastic properties spanned by the Voigt and Reuss bounds is comparatively large and depend on the degree of anisotropy of the monocrystal. This procedure therefore does not necessarily lead to useful estimates. In present work it is our concern to introduce tighter bounds by introducing a more sophisticated homogenization approach. Thereby we restrict ourselves to second-order estimates. Such more precise bounds for the effective elastic behavior are the Hashin-Shtrikman bounds (Hashin and Shtrikman, 1962a,b). They are derived from a variational principle, which is formulated for stress polarization and is based on the introduction of a homogeneous comparison material. In contrast to the estimates by Voigt and Reuss these bounds are based on the solution of a boundary value problem. The solution is obtained by means of Green's functions. By the appropriate choice of the stiffness of the reference material, one obtains an upper or a lower bound for the effective properties. We here determine these bounds for cubic crystal aggregates in case of an isotropic orientation distribution. While considering a homogeneous and isotropic material for the polycrystal, a variational problem is derived which results in bounds of the effective material parameters of the heterogeneous aggregate.

1.2 Procedure

The outline of this paper is as follows. In the second section, the constitutive relations for both, a single crystal and the crystal aggregate are introduced. The rational representation of constitutive measures is based on the projector representation. Furthermore, the theoretical foundations of Hashin-Shtrikman variational principle are reproduced exploiting the aggregate-specific macroscopic isotropy of poly-Si. The explanations are closely tied to the works by Hashin and Shtrikman (1962a,b, 1963), Walpole (1966a,b), and Willis (1977, 1981). For the subsequent determination of the respective bounds, eigenvalues of the constitutive measures are utilized. In the third section, the procedure introduced here is applied to particular initial parameters for silicon. These values are analyzed and the degree of anisotropy of the starting material is discussed. The bounds for the effective material behavior are presented and a measure for the bandwidth of the bounds is introduced. Moreover, in the fourth section, the results obtained are compared to results of a preceding publication where the first-order bounds were identified. Additionally, experimental results, representing the behavior of the poly-Si aggregate, are examined which provide comparison data for the homogenization results.

* E-mail address: marcus.assmus@ovgu.de
doi: 10.24352/UB.OVGU-2021-004

The different bounds for the effective stiffness components and also for engineering parameters have been investigated. Measures for the deviation from a real material are introduced and discussed and the degree of improvement of the bounds compared to first-order estimates is highlighted. All results are illustrated concisely. The fifth section is dedicated to the improvements and problems in the context of the present investigations. The main outcomes are summarized in the closing section. Strategies for the generation of improved solutions are outlined there.

1.3 Notation

In the present paper, a direct tensor notation is applied. Light slanted letters, e.g. a or A, indicate scalar quantities. First and second-order tensors are denoted by lower or upper case bold letters, respectively, e.g. $\boldsymbol{a}$ or $\boldsymbol{A}$. Fourth-order tensors are represented by upper case blackboard-bold letters, e.g. $\mathbb{A}$. The scalar and the dyadic products are denoted by $\boldsymbol{A}\cdot\boldsymbol{B}$ and $\boldsymbol{A}\otimes\boldsymbol{B}$. A linear mapping is denoted by $\boldsymbol{A}=\mathbb{C}\colon\boldsymbol{B}$ and a fourfold contraction is by $\mathbb{B}\colon\colon\mathbb{B}=B$. Tensorial quantities enclosed in double strokes represent the Frobenius norm, i.e. for fourth-order tensors $\|\mathbb{C}\|=[\mathbb{C}\colon\colon\mathbb{C}]^{1/2}$ holds. Moreover, we make use of the Rayleigh product $\boldsymbol{B}\star\mathbb{C}^0=\mathbb{C}$ which maps all basis vectors of $\mathbb{C}^0$ simultaneously without changing its components. The tensor $\boldsymbol{I}$ is the identity on vectors. The identity on tensors of second-order is given by $\mathbb{I}$. The symbol 'div' is used for the three-dimensional divergence operator. Quantities superimposed with a tilde, a hat, or a bar denote fluctuating, auxiliary or effective parameters.

2 Theory

2.1 Origin and objective

The starting point of our venture is the constitutive law for a single crystal. For silicon, a linear elastic relation is reasonable, i.e. we make use of Hooke's law in the form

$$\boldsymbol{T}(\boldsymbol{x})=\mathbb{C}(\boldsymbol{x})\colon\boldsymbol{E}(\boldsymbol{x}) \tag{1}$$

with Cauchy stress tensor $\boldsymbol{T}$ and linearized strain tensor $\boldsymbol{E}$, while the stiffness tensor for cubic symmetry is determined as follows when we leave the location-dependency unrecorded.

$$\mathbb{C}^{\mathrm{c}}=\lambda_1^{\mathrm{c}}\mathbb{P}_1^{\mathrm{c}}+\lambda_2^{\mathrm{c}}\mathbb{P}_2^{\mathrm{c}}+\lambda_3^{\mathrm{c}}\mathbb{P}_3^{\mathrm{c}} \tag{2}$$

Herein we have introduced cubic eigenvalues (Sutcliffe, 1992)

$$\lambda_1^{\mathrm{c}}=C_{1111}+2C_{1122},\qquad \lambda_2^{\mathrm{c}}=C_{1111}-C_{1122},\qquad \lambda_3^{\mathrm{c}}=2C_{2323}\,, \tag{3}$$

and cubic eigenprojectors (Rychlewski, 1995)

$$\mathbb{P}_1^{\mathrm{c}}=\frac{1}{3}\,\boldsymbol{I}\otimes\boldsymbol{I}\,,\qquad \mathbb{P}_2^{\mathrm{c}}=\mathbb{D}-\mathbb{P}_1^{\mathrm{c}}\,,\qquad \mathbb{P}_3^{\mathrm{c}}=\mathbb{I}^{\mathrm{sym}}-\left(\mathbb{P}_1^{\mathrm{c}}+\mathbb{P}_2^{\mathrm{c}}\right)\,, \tag{4}$$

while

$$\mathbb{D}=\sum_{i=1}^{3}\boldsymbol{g}_i\otimes\boldsymbol{g}_i\otimes\boldsymbol{g}_i\otimes\boldsymbol{g}_i=\boldsymbol{Q}\star\mathbb{D}^0\quad\text{with}\quad\mathbb{D}^0=\sum_{i=1}^{3}\boldsymbol{e}_i\otimes\boldsymbol{e}_i\otimes\boldsymbol{e}_i\otimes\boldsymbol{e}_i\,, \tag{5}$$

is the anisotropic portion, and $2\mathbb{I}^{\mathrm{sym}}=\boldsymbol{e}_i\otimes\boldsymbol{e}_j\otimes\left(\boldsymbol{e}_i\otimes\boldsymbol{e}_j+\boldsymbol{e}_j\otimes\boldsymbol{e}_i\right)$ is the identity on symmetric second-order tensors. Here we make use of the orientation $\boldsymbol{Q}\in\mathcal{SO}_3$ of the single crystal, that maps the basis $\{\boldsymbol{e}_i\}$ onto the crystallographic basis $\{\boldsymbol{g}_i\}$, i.e. $\boldsymbol{Q}=\boldsymbol{g}_i\otimes\boldsymbol{e}_i$. To relate the cubic eigenvalues to tangible quantities, the bulk modulus K and the two shear moduli $G_\beta^{\mathrm{c}}\ \forall\,\beta\in\{1,2\}$ of a cubic crystal are given as follows.

$$\lambda_1^{\mathrm{c}}=3K^{\mathrm{c}}\qquad \lambda_2^{\mathrm{c}}=2G_1^{\mathrm{c}}\qquad \lambda_3^{\mathrm{c}}=2G_2^{\mathrm{c}} \tag{6}$$

The effective medium based on the polycrystalline aggregate to be determined is homogeneous, i.e. the location-dependency of the elastic properties vanishes ($\mathbb{C}\neq f(\boldsymbol{x})$). As a result, Hooke's law reads

$$\boldsymbol{T}(\boldsymbol{x})=\overline{\mathbb{C}}\colon\boldsymbol{E}(\boldsymbol{x}) \tag{7}$$

where $\overline{\mathbb{C}}$ is the effective constitutive tensor for arbitrary material points $\boldsymbol{x}$. As introduced in the preface, the effective elasticity is assumed to be isotropic, i.e. $\overline{\mathbb{C}}\equiv\mathbb{C}^{\circ}$. We can then write the constitutive tensor of the isotropic approximation as (Rychlewski, 1995)

$$\mathbb{C}^{\circ}=\lambda_1^{\circ}\mathbb{P}_1^{\circ}+\lambda_2^{\circ}\mathbb{P}_2^{\circ} \tag{8}$$

where for the isotropic eigenvalues

$$\lambda_1^{\circ}=3K\qquad\text{and}\qquad\lambda_2^{\circ}=2G \tag{9}$$

hold, while G and K are the isotropic bulk and shear moduli. The associated isotropic projectors are as follows (Rychlewski, 1995).

$$\mathbb{P}_1^\circ = \mathbb{P}_1^{\mathrm{c}} \qquad\qquad \mathbb{P}_2^\circ = \mathbb{I}^{\mathrm{sym}} - \mathbb{P}_1^\circ \tag{10}$$

An isotropic stiffness as introduced in Eq. (8) can be expressed by a cubic stiffness tensor also.

$$\mathbb{C}^\circ = \lambda_1^{\mathrm{c}}\mathbb{P}_1^{\mathrm{c}} + \lambda_2^\circ\mathbb{P}_2^{\mathrm{c}} + \lambda_2^\circ\mathbb{P}_3^{\mathrm{c}} \tag{11}$$

This reveals the isotropy condition $\lambda_2^\circ = \lambda_2^{\mathrm{c}} = \lambda_3^{\mathrm{c}}$. With respect to Eq. (6), this condition thus becomes $G = G_1^{\mathrm{c}} = G_2^{\mathrm{c}}$. Zener (1948) established a measure to indicate the degree of anisotropy, the so-called Zener ratio, which can be formulated in terms of the cubic eigenvalues so that $\lambda_3^{\mathrm{c}} - \lambda_2^{\mathrm{c}} = \lambda_2^{\mathrm{c}}(\mathcal{Z}R - 1)$ applies ($\mathcal{Z}R > 0$ since $\lambda_J^{\mathrm{c}} > 0$ holds). Obviously, $\mathcal{Z}R = 1$ indicates isotropic material behavior. In contrast, we can formulate the cubic stiffness in terms of isotropic projectors.

$$\mathbb{C}^{\mathrm{c}} = \left(\lambda_1^{\mathrm{c}} - \lambda_2^{\mathrm{c}} + \lambda_3^{\mathrm{c}}\right)\mathbb{P}_1^\circ + \lambda_3^{\mathrm{c}}\mathbb{P}_2^\circ + (\lambda_2^{\mathrm{c}} - \lambda_3^{\mathrm{c}})\boldsymbol{Q} \star \mathbb{D}^0 \tag{12}$$

Obviously, $\mathbb{C}^{\mathrm{c}}$ turns $\mathbb{C}^\circ$ when $\lambda_2^{\mathrm{c}} = \lambda_3^{\mathrm{c}}$ holds.

2.2 Hashin-Shtrikman bounds for crystalline aggregate

The determination of effective properties of inhomogeneous materials is a long standing problem. The methodology introduced hereinafter is valid for polycrystals consisting of linear elastic crystals with cubic material symmetry, which are not subject to any texture. As announced, we confine our considerations to second-order estimates for the effective behavior related to the approach originally introduced by Hashin and Shtrikman (1962a,b). We now consider a homogeneous problem of comparison

$$\boldsymbol{T}^0 = \mathbb{C}^0 \colon \boldsymbol{E}^0 \,, \tag{13}$$

where $\mathbb{C}^0$ is a homogeneous stiffness. Hereinafter, all quantities indexed with 0 are location-independent. Hashin and Shtrikman (1962a,b) construct a functional for the difference problem

$$\delta\boldsymbol{T}(\boldsymbol{x}) = \boldsymbol{T}(\boldsymbol{x}) - \boldsymbol{T}^0 \tag{14}$$

which

- leads to the principle of minimum complementary energy for $\mathbb{C}^0 \to 0$,
- leads to the principle of minimum potential energy for $\mathbb{C}^0 \to \infty$,
- takes the value of the effective elastic energy in the place of the solution,
- and is a minimum or a maximum depending on the choice of $\mathbb{C}^0$.

Due to the last point mentioned, the procedure based on the works of Hashin and Shtrikman leads to bounds analogous to Voigt-Reuss bounds as introduced for present problem in Aßmus et al. (2020). These improved bounds, however, are tighter due to the following reasons:

- The value of the functional can be adjusted with $\mathbb{C}^0$.
- The initial state is a homogeneously deformed representative volume element, which is closer to the real solution than the undeformed representative volume element (Voigt) or the stress-free representative volume element (Reuss).
- The factual bounds are defined by more complex approaches compared to the ones obtained by homogeneous deformations (Voigt) or homogeneous stresses (Reuss).

Considering the difference problem, we reformulate Eq. (14)

$$\boldsymbol{T}(\boldsymbol{x}) = \mathbb{C}^0 \colon \boldsymbol{E}(\boldsymbol{x}) + \left[\mathbb{C}(\boldsymbol{x}) - \mathbb{C}^0\right] \colon \boldsymbol{E}(\boldsymbol{x}) \tag{15}$$

and introduce the heterogeneous polarization stress tensor $\boldsymbol{P}$. This equation then takes the form

$$\boldsymbol{T}(\boldsymbol{x}) = \mathbb{C}^0 \colon \boldsymbol{E}(\boldsymbol{x}) + \boldsymbol{P}(\boldsymbol{x}) \qquad \text{with } \boldsymbol{P}(\boldsymbol{x}) = \delta\mathbb{C}(\boldsymbol{x}) \colon \boldsymbol{E}(\boldsymbol{x}) \,. \tag{16}$$

The boundary problem is involving an inhomogeneous material without body forces.

$$\operatorname{div}\left[\boldsymbol{T}(\boldsymbol{x})\right] = \operatorname{div}\left[\mathbb{C}^0 \colon \boldsymbol{E}(\boldsymbol{x})\right] + \operatorname{div}\left[\boldsymbol{P}(\boldsymbol{x})\right] = \boldsymbol{o} \tag{17}$$

The strains solving this boundary value problem are given by subsequent expression if the polarization would be known.

$$\boldsymbol{E}(\boldsymbol{x}) = \boldsymbol{E}^0 - \mathbb{G}(\boldsymbol{x}) \colon \boldsymbol{P}(\boldsymbol{x}) \tag{18}$$

Herein $\boldsymbol{E}_0$ is the reference strain and $\mathbb{G}$ is the integral operator acting

$$\mathbb{G}(\boldsymbol{x}) \colon \boldsymbol{P}(\boldsymbol{x}) = \int_{V'} \mathbb{L}(\boldsymbol{x} - \boldsymbol{x}') \colon \boldsymbol{P}(\boldsymbol{x}') \, \mathrm{d}V' \tag{19}$$

with the property (Kunin, 1981)

$$\mathbb{G}(\boldsymbol{x}) : \boldsymbol{P}(\boldsymbol{x}) = \mathbb{G}(\boldsymbol{x}) : \left[\boldsymbol{P}(\boldsymbol{x}) - \frac{1}{V} \int_V \boldsymbol{P}(\boldsymbol{x}) \, \mathrm{d}V \right] . \tag{20}$$

Therein, the fourth-order tensor $\mathbb{L}$ is determined by

$$\mathbb{L}(\boldsymbol{x} - \boldsymbol{x}') = -\frac{1}{4} \left[\frac{\partial^2 G_{ij}}{\partial x_k \partial x_n} + \frac{\partial^2 G_{ik}}{\partial x_j \partial x_n} + \frac{\partial^2 G_{nj}}{\partial x_k \partial x_i} + \frac{\partial^2 G_{nk}}{\partial x_j \partial x_i} \right] \boldsymbol{e}_i \otimes \boldsymbol{e}_n \otimes \boldsymbol{e}_j \otimes \boldsymbol{e}_k \tag{21}$$

which includes the second derivatives of infinite body's Green's function $\boldsymbol{G} = \boldsymbol{G}(\boldsymbol{x} - \boldsymbol{x}')$, cf. Kröner (1972); Dederichs and Zeller (1972); Zeller and Dederichs (1973).
The polarization fulfilling the boundary value problem is given as a solution of subsequent form.

$$\delta\mathbb{C}^{-1}(\boldsymbol{x}) : \boldsymbol{P}(\boldsymbol{x}) + \mathbb{G}(\boldsymbol{x}) : \boldsymbol{P}(\boldsymbol{x}) = \boldsymbol{E}^0 \tag{22}$$

Equation (22) is equivalent to the variational principle

$$\delta\mathcal{F} = \delta \left[\frac{1}{2} \boldsymbol{P}(\boldsymbol{x}) : \delta\mathbb{C}^{-1} : \boldsymbol{P}(\boldsymbol{x}) + \frac{1}{2} \boldsymbol{P}(\boldsymbol{x}) : \mathbb{G} : \boldsymbol{P}(\boldsymbol{x}) - \boldsymbol{P}(\boldsymbol{x}) : \boldsymbol{E}^0 \right] \tag{23}$$

or more compact

$$\delta\mathcal{F} = \left[\delta\mathbb{C}^{-1} : \boldsymbol{P}(\boldsymbol{x}) + \mathbb{G} : \boldsymbol{P}(\boldsymbol{x}) - \boldsymbol{E}^0 \right] : \boldsymbol{P}(\boldsymbol{x}) \, . \tag{24}$$

The volume average of Eq. (23) needs to reach stationarity when considering heterogeneous materials, i.e.

$$\delta\hat{\mathcal{F}} = \int_V \delta\mathcal{F} \mathrm{d}V = 0 \, , \tag{25}$$

so that $\hat{\mathcal{F}} = W^0 - \hat{W}$ holds, cf. Willis (1977). Herein, W^0 is the strain energy of the homogeneous comparison material and $\hat{W}$ is the effective strain energy of the heterogeneous material. The second derivative $\delta\delta\hat{\mathcal{F}}$ provides information on $\hat{\mathcal{F}}$ being minimum or maximum.

$$\delta\delta\hat{\mathcal{F}} = \int_V \delta\boldsymbol{P} : \left[\delta\mathbb{C}^{-1}(\boldsymbol{x}) + \mathbb{G}(\boldsymbol{x}) \right] : \delta\boldsymbol{P} \, \mathrm{d}V \qquad \begin{cases} > 0 & \hat{\mathcal{F}} \triangleq \min \\ < 0 & \hat{\mathcal{F}} \triangleq \max \end{cases} \tag{26}$$

The operator appearing in Eq. (26) was examined by Willis (1977) and he showed that if $\delta\mathbb{C}$ is positive (negative) definite, then $\delta\mathbb{C}^{-1}(\boldsymbol{x}) + \mathbb{G}(\boldsymbol{x})$ is positive (negative) definite also. From the Hashin-Shtrikman functional $\hat{\mathcal{F}} = W^0 - \hat{W}$ we can conclude

$$\delta\mathbb{C} \begin{cases} \text{positive definite:} & \delta\delta\bar{\mathcal{F}} > 0, \hat{W} = \hat{W}_{\max} \\ \text{negative definite:} & \delta\delta\bar{\mathcal{F}} < 0, \hat{W} = \hat{W}_{\min} \end{cases} . \tag{27}$$

Nadeau and Ferrari (2001) showed that optimal bounds are found if $\mathbb{C}^0$ is isotropic. When applying the method proposed by them, the Hashin-Shtrikman bounds must be obtained for

$$\mathbb{C}_0^{\mathrm{HS}\pm} = \lambda_1^{\mathrm{HS}\pm} \mathbb{P}_1^\circ + \lambda_2^{\mathrm{HS}\pm} \mathbb{P}_2^\circ \tag{28}$$

with $\lambda_1^{\mathrm{HS}+} = \lambda_1^{\mathrm{HS}-}$, $\lambda_2^{\mathrm{HS}+} = \max(\lambda_2, \lambda_3)$, and $\lambda_2^{\mathrm{HS}-} = \min(\lambda_2, \lambda_3)$ for upper and lower bounds indicated by HS+ and HS-.
As discussed by Willis (1977, 1981), for the special conditions utilized as assumptions for present investigations, $\mathbb{G}$ becomes Hills polarization tensor $\mathbb{P}_0$, cf. Hill (1965); Mura (1987),

$$\mathbb{P}_0 = \frac{1}{4\pi} \iint_{\partial S} \mathbb{H}(\mathbb{C}, \boldsymbol{n}) \, \mathrm{d}S(\boldsymbol{n}) \tag{29}$$

with

$$\mathbb{H} = \frac{2\lambda_1^\circ + \lambda_2^\circ}{\lambda_2^\circ (\lambda_1^\circ + 2\lambda_2^\circ)} \boldsymbol{n} \otimes \boldsymbol{n} \otimes \boldsymbol{n} \otimes \boldsymbol{n} + \frac{1}{\lambda_2^\circ} \mathbb{I}^{\mathrm{sym}} : (\boldsymbol{I} \boxtimes (\boldsymbol{n} \otimes \boldsymbol{n})) : \mathbb{I}^{\mathrm{sym}} \tag{30}$$

where $\mathrm{d}S$ is a surface element of the unit sphere S and

$$\boldsymbol{I} \boxtimes (\boldsymbol{n} \otimes \boldsymbol{n}) = \delta_{ij} n_k n_l \boldsymbol{e}_i \otimes \boldsymbol{e}_l \otimes \boldsymbol{e}_j \otimes \boldsymbol{e}_k$$

is the outer product. This form of Hills polarization tensor is well known, cf. Willis (1977, 1981); Castañeda and Suquet (1997).
The strain localization eliminating $\boldsymbol{E}^0$ leads to a modification of Eq. (18), so that

$$\boldsymbol{E}(\boldsymbol{x}) = \left(\mathbb{I}^{\mathrm{sym}} + \mathbb{G} : \delta\mathbb{C} \right)^{-1} : \boldsymbol{E}^0 \tag{31}$$

Tab. 1: Eigenvalues for a Si monocrystal (Hosford, 1993)

λ_J^{c}	$J=1$	$J=2$	$J=3$
$[\mathrm{N/mm^2}]$	$295.00 \cdot 10^3$	$101.80 \cdot 10^3$	$159.40 \cdot 10^3$

The generalized Hashin-Shtrikman stiffness tensor is then given as follows, cf. Willis (1977).

$$\bar{\mathbb{C}}^{\mathrm{HS}\pm} = \int_V \mathbb{C} \left(\mathbb{I}^{\mathrm{sym}} + \mathbb{P}_0 : \delta\mathbb{C}^{\mathrm{HS}\pm} \right)^{-1} \left[\int_V \left(\mathbb{I}^{\mathrm{sym}} + \mathbb{P}_0 : \delta\mathbb{C}^{\mathrm{HS}\pm} \right)^{-1} \mathrm{d}V \right]^{-1} \mathrm{d}V \tag{32}$$

For such an isotropic effective stiffness, upper and lower bound of the first eigenvalue coincide, i.e. in case of cubic crystal symmetry, the spherical eigenvalue of the bounds determined equals the spherical eigenvalue of the single crystal. It is thus necessary to consider the computation of the second eigenvalue, only. The eigenvalues are determined by subsequent expressions, valid for the case $\lambda_3^{\mathrm{c}} > \lambda_2^{\mathrm{c}}$.

$$\bar{\lambda}_1^{\mathrm{HS}\pm} = \lambda_1^{\mathrm{c}} \tag{33}$$

$$\bar{\lambda}_2^{\mathrm{HS}+} = \lambda_3^{\mathrm{c}} + 2 \left[\frac{5}{\lambda_2^{\mathrm{c}} - \lambda_3^{\mathrm{c}}} + \frac{6 \quad (\lambda_1^{\mathrm{c}} + 3\lambda_3^{\mathrm{c}})}{5\lambda_3^{\mathrm{c}}(\lambda_1^{\mathrm{c}} + 2\lambda_3^{\mathrm{c}})} \right]^{-1} \tag{34}$$

$$\bar{\lambda}_2^{\mathrm{HS}-} = \lambda_2^{\mathrm{c}} + 3 \left[\frac{5}{\lambda_3^{\mathrm{c}} - \lambda_2^{\mathrm{c}}} + \frac{4 \quad (\lambda_1^{\mathrm{c}} + 3\lambda_2^{\mathrm{c}})}{5\lambda_2^{\mathrm{c}}(\lambda_1^{\mathrm{c}} + 2\lambda_2^{\mathrm{c}})} \right]^{-1} \tag{35}$$

However, when comparing stiffnesses derived here to first-order bounds determined in Aßmus et al. (2020), one may conclude subsequent relations with the inequality understood in the spectral sense.

$$\mathbb{C}^{\mathrm{V}} \geq \bar{\mathbb{C}}^{\mathrm{HS}+} \geq \bar{\mathbb{C}}^{\mathrm{HS}-} \geq \mathbb{C}^{\mathrm{R}} \tag{36}$$

Herein, the upper indexes V and R indicate Voigt and Reuss bounds.

3 Application and Discussion

The Hashin-Shtrikman bounds are now evaluated with the set of material parameters given in Tab. 1. Therein, the original values C_{ijkl} given in Hosford (1993) are converted into eigenvalues λ_J^{c} according to Eq. (11). Obviously, $\lambda_2^{\mathrm{c}} < \lambda_3^{\mathrm{c}}$ holds. The Zener ratio is $ZR = 1.57$. As compared with other cubic materials in Aßmus et al. (2020), this degree of anisotropy is moderate.
When applying the procedure described in Sect. 2.2, material parameters given in Tab. 2 result. The bandwidth spanned by the second eigenvalues of the isotropic effective bounds is $\Delta\lambda_2^{\mathrm{HS}\pm} = |\lambda_2^{\mathrm{HS}+} - \lambda_2^{\mathrm{HS}-}| = 570\,\mathrm{N/mm^2}$.
Hashin-Shtrikman bounds lead to improved bounds of effective material parameters. These improvements relate to first-order bounds associated with the names Voigt (1910) and Reuss (1929). Here-named bounds should be included in the discussion to illustrate the degree of improvement. As was derived in Aßmus et al. (2020), the eigenvalues of Voigt and Reuss isotropic bounds are determined as follows.

$$\lambda_1^{\mathrm{V}} = \lambda_1^{\mathrm{c}} \qquad \lambda_1^{\mathrm{R}} = \lambda_1^{\mathrm{c}} \tag{37}$$

$$\lambda_2^{\mathrm{V}} = \frac{2}{5}\lambda_2^{\mathrm{c}} + \frac{3}{5}\lambda_3^{\mathrm{c}} \qquad \lambda_2^{\mathrm{R}} = \left[\frac{2}{5}\frac{1}{\lambda_2^{\mathrm{c}}} + \frac{3}{5}\frac{1}{\lambda_3^{\mathrm{c}}} \right]^{-1} \tag{38}$$

These eigenvalues are related to isotropic Voigt and Reuss stiffnesses.

$$\mathbb{C}^{\square} = \lambda_1^{\square}\mathbb{P}_1^{\circ} + \lambda_2^{\square}\mathbb{P}_2^{\circ} \qquad \forall\, \square \in \{\mathrm{V}, \mathrm{R}\} \tag{39}$$

Tab. 2: Analytically determined Hashin-Shtrikman bounds of eigenvalues for poly-Si

$\lambda_J^{\square}$	$J=1, \square = \mathrm{HS}\pm$	$J=2, \square = \mathrm{HS}+$	$J=2, \square = \mathrm{HS}-$
$[\mathrm{N/mm^2}]$	$295.00 \cdot 10^3$	$133.53 \cdot 10^3$	$132.96 \cdot 10^3$

Tab. 3: Eigenvalues of Voigt and Reuss bounds for poly-Si (Aßmus et al., 2020)

$\lambda_J^{\square}$	$J=1, \square = \mathrm{V} \vee \mathrm{R}$	$J=2, \square = \mathrm{V}$	$J=2, \square = \mathrm{R}$
$[\mathrm{N/mm^2}]$	$295.00 \cdot 10^3$	$136.36 \cdot 10^3$	$129.98 \cdot 10^3$

Again we can identify $\lambda_1^{\mathrm{HS}\pm} = \lambda_1^{\mathrm{R}} = \lambda_1^{\mathrm{V}} = \lambda_1^{\mathrm{c}}$. Results are given in Tab. 3.
For comparison we use experimental data from Michalicek et al. (1995) and Sharpe et al. (1997) compiled in Tab. 4. Based on the experimental findings, we can introduce the experimentally determined isotropic stiffness tensor of the polycrystalline aggregate.

$$\mathbb{C}^{\mathrm{exp}} = \lambda_1^{\mathrm{exp}} \mathbb{P}_1^{\circ} + \lambda_2^{\mathrm{exp}} \mathbb{P}_2^{\circ} \tag{40}$$

In a first step we plot the eigenvalue relations $\dfrac{\lambda_\alpha}{\lambda_1}\ \forall\ \alpha = \{2,3\}$ of present findings, the initial data and the experimental results as an analogue to the well-known Blackwell diagram, cf. Blackman (1938). Here, two dimensionless ratios of elastic constants are used for visualization purposes. Clearly, in the case of isotropy $\dfrac{\lambda_3}{\lambda_1} = \dfrac{\lambda_2}{\lambda_1}$ holds. We can find Zeners ratio via the reciprocally proportional function

$$\frac{\lambda_2}{\lambda_1} = \frac{1}{ZR}\,\frac{\lambda_3}{\lambda_1}\,. \tag{41}$$

With increasing Zener ratio, the slope of this function decreases. The isotropic function, which is containing homogenized and experimental results in present case, is bisecting the functional area. Again, Hashin-Shtrikman bounds lie between Voigt and Reuss bounds. The experimental results are, however, out of this range. As a common measure for such a gap, we can introduce subsequent distances.

$$d^{\square} = \frac{\|\mathbb{C}^{\square} - \mathbb{C}^{\mathrm{exp}}\|}{\|\mathbb{C}^{\mathrm{exp}}\|} \qquad \forall\ \square \in \{\mathrm{V}, \mathrm{R}, \mathrm{HS}+, \mathrm{HS}-\} \tag{42}$$

These distances are given Fig. 1 on the right-hand side. As already evident, the Voigt bound has the smallest distance to the experimental findings. The opposite applies to the Reuss bound. Hashin-Shtrikman bounds lie inbetween Voigt-Reuss bounds while the upper Hashin-Shtrikman bound HS+ is closer to experiments. The upper bounds of the effective characteristics (V, HS+) show the respective smaller distances, the lower bounds (R, HS-) reveal the respective larger ones.
We additionally analyze the bandwidths spanned by the respective upper and lower bounds, i.e. $\Delta d^{\mathrm{VR}} = |d^{\mathrm{V}} - d^{\mathrm{R}}| = 2.259 \cdot 10^{-2}$ and $\Delta d^{\mathrm{HS}\pm} = |d^{\mathrm{HS}+} - d^{\mathrm{HS}-}| = 2.32 \cdot 10^{-3}$. These bandwidths are indicated by gray shadings at in the diagram on the right-hand side of Fig. 1. Even when all bounds determined are somehow distant to experimental findings, these bandwidths indicate an improvement of the theoretical considerations following the introduction of second-order estimates by the Hashin-Shtrikman based procedure, i.e. $\Delta d^{\mathrm{VR}} > \Delta d^{\mathrm{HS}\pm}$. When considering the ratio $\dfrac{\Delta d^{\mathrm{HS}\pm}}{\Delta d^{\mathrm{VR}}} \approx 0.103$ we obtain a reduction of the bandwidth by about 90% compared to first-order bounds.
To complete the investigations, we compare isotropic engineering parameters, i.e. we make use of the couples consisting of the bulk modulus K together with the shear modulus G

$$K^{\square} = \frac{1}{3}\lambda_1^{\square} \qquad G^{\square} = \frac{1}{2}\lambda_2^{\square} \qquad \forall\ \square \in \{\mathrm{V}, \mathrm{R}, \mathrm{HS}+, \mathrm{HS}-, \mathrm{exp}\}\,, \tag{43}$$

and the Young's modulus Y together with the Poisson's ratio ν

$$Y^{\square} = \frac{3\lambda_1^{\square}\lambda_2^{\square}}{2\lambda_1^{\square} + \lambda_2^{\square}} \qquad \nu^{\square} = \frac{\lambda_1^{\square} - \lambda_2^{\square}}{2\lambda_1^{\square} + \lambda_2^{\square}} \qquad \forall\ \square \in \{\mathrm{V}, \mathrm{R}, \mathrm{HS}+, \mathrm{HS}-, \mathrm{exp}\}\,, \tag{44}$$

Tab. 4: Experimentally determined values of poly-Si (Michalicek et al., 1995; Sharpe et al., 1997)

λ_J^{exp}	$J=1$	$J=2$
$[\mathrm{N/mm^2}]$	$291.07 \cdot 10^3$	$133.60 \cdot 10^3$

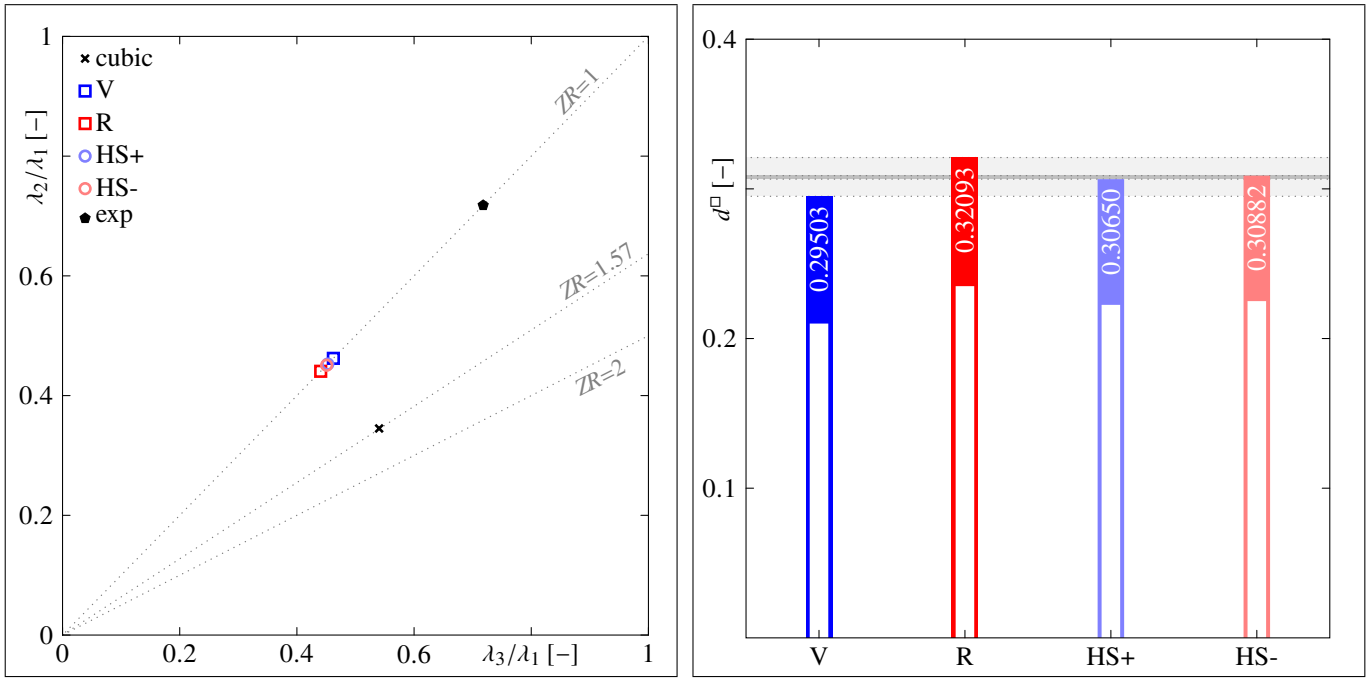

Fig. 1: Relations for eigenvalue ratio (left) and distances of bounds to experimental findings (right)

for all homogenization procedures applied here and in Aßmus et al. (2020), as well as for the experimental findings. The results are plotted in Fig. 2. On the left-hand side we find the representation where bulk and shear moduli are related. All homogenization results of course feature the same bulk modulus. Also here the bounds of the homogenization in terms of shear moduli are clearly visible. In sortation of magnitude, these are G^{V}, G^{HS+}, G^{HS-}, and G^{R}. The experimental findings, however, have a slightly different bulk modulus and and a strongly deviating shear modulus. Note that the experimental data is found at lower bulk moduli but at higher shear moduli compared to all estimates determined here. On the opposite side, we find a representation for Young's modulus and Poisson's ratio. Therein, it is evident that these experimental results are at least within the range spanned by the Voigt and Reuss bounds (light gray). However, the experiments are outside the range spanned by the Hashin-Shtrikman bounds (dark gray). Considering Young's modulus solely, the experimental findings fit very well, since they are within the Hashin-Shtrikman bounds. This is not the case for Poisson's ratio, since the experiment yields much smaller values. Considering the diagonal of the area spanned by the Voigt and Reuss bounds, the experiments lie below this line, i.e. effective Young's modulus and Poisson's ratio are in the upper left triangle of the quadrangle specified by the bounds. To complete the presentation of the results we give the engineering values for all homogenization processes and the experiment in Tab. 5. The arithmetic mean of first-order estimates, usually referred to as Hill approximation (Hill, 1952), can be determined by

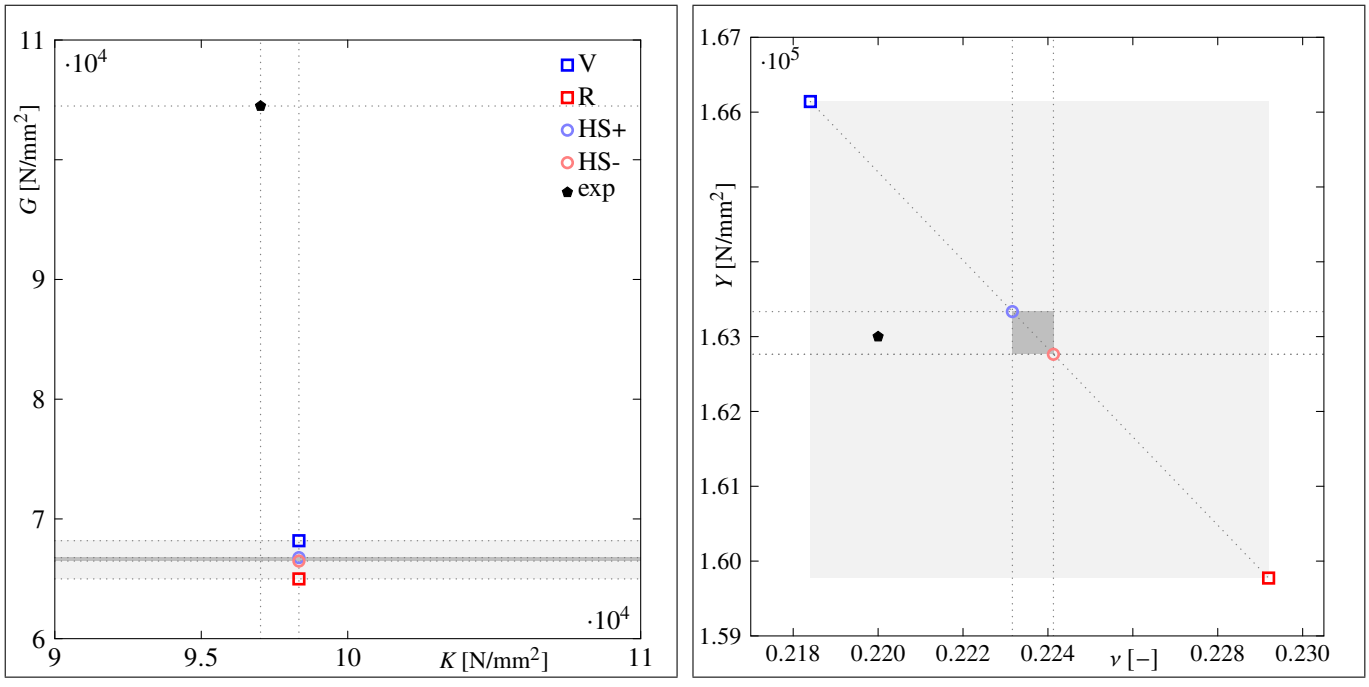

Fig. 2: Comparison for bulk and shear modulus as well as Young's modulus and Poisson's ratio

Tab. 5: Engineering parameters of bounds determined here in comparison to experimental findings

$\square$	$K^{\square}$ [N/mm²]	$G^{\square}$ [N/mm²]	$Y^{\square}$ [N/mm²]	$\nu^{\square}$ [−]
V	$98.33 \cdot 10^3$	$68.18 \cdot 10^3$	$166.14 \cdot 10^3$	0.218
R	$98.33 \cdot 10^3$	$64.99 \cdot 10^3$	$159.77 \cdot 10^3$	0.229
H	$98.33 \cdot 10^3$	$66.59 \cdot 10^3$	$162.97 \cdot 10^3$	0.224
HS+	$98.33 \cdot 10^3$	$66.77 \cdot 10^3$	$163.33 \cdot 10^3$	0.223
HS-	$98.33 \cdot 10^3$	$66.48 \cdot 10^3$	$162.76 \cdot 10^3$	0.224
exp	$97.02 \cdot 10^3$	$104.49 \cdot 10^3$	$163.00 \cdot 10^3$	0.220

the aid of the Voigt-Reuss bounds, i.e. $\lambda_2^{\mathrm{H}} = \frac{1}{2}\left[\lambda_2^{\mathrm{V}} + \lambda_2^{\mathrm{R}}\right]$ while the coincidence $\lambda_1^{\mathrm{H}} = \lambda_1^{\mathrm{c}}$ holds, cf. Aßmus et al. (2020). This Hill estimate finds broad practical application, cf. e.g. Nabavi et al. (2017). We have also added this value to the overview in above table. However, the resulting value obviously lies within the Hashin-Shtrikman bounds in context of shear modulus and Young's modulus. The engineering parameters based on this estimate are determined by the relations given in Eqs. (43) and (44), too.

4 Conclusion

As can be seen in Fig. 2, the effort to apply an advanced theory to determine tighter bounds has been worthwhile from a theoretical point of view. We conclude that the improved bounds presented through Hashin-Shtrikman variational formulation are significantly tighter than the Voigt-Reuss bounds. Indeed, these are the tightest possible bounds for isotropic aggregates.

A comparison of present predictions with the experimental data shows that the values of elasticity parameters strongly depends on the type of the evaluation. Although the homogenization of the effective quantities is based on the eigenvalues, the experimental data for directly derived quantities (K, G) lies far outside the bounds determined. The counterpart is the evaluation in terms of classical engineering parameters (Y, ν), whereby experimental results fit better within the determined bounds. This is particularly true for the Young's modulus. A deviation from the range of the specified bounds is detected for the Poisson's ratio.

Besides metrological problems of resolution and accuracy, this deviation may be a result of the constituents forming the aggregate. So far, the influence of the crystallographic and the morphological anisotropy of the aggregate on the macroscopic elastic response remain unconsidered. Thus size, shape, arrangement, and distributions of the crystals are neglected. Thus, the discrepancies revealed here could be due to

- correlations between the crystal orientation and crystal shape,
- correlations between the crystal orientations of neighboring crystals, or
- imperfections at the interface between crystals.

5 Closure

In present work, the Hashin-Shtrikman bounds for physically linear problems of polycrystalline aggregates consisting of cubic monocrystals is reviewed, discussed and applied to poly-Si for use at solar cells. Compared to classical studies on the subject, e.g. Hopcroft et al. (2010), we were able to substantially bound the theoretically possible range of the elastic behavior of polycrystalline silicon. This improvement was achieved by the application of the Hashin-Shtrikman variational formulation for polycrystals. Thereby, The examination of the elastic properties of poly-Si has been carried out by using analytical estimates solely. These are a considerable improvement compared to Voigt-Reuss bounds. However, it is apparent that predicting the effective elastic behavior of poly-Si SC's precisely is non-trivial. The experimentally determined parameters violate the Hashin-Shtrikman bounds, cf. Fig. 2. This is often related to the problem, that the basic assumptions of the homogenization procedure are not fulfilled. On the other hand, the accuracy of the experimental results must be contested.

Finally, the more information on the statistical distribution of the crystals of the heterogeneous material is available, the more precise the real material behavior can be predicted. Thus, a modified analytical procedure incorporating morphological and

crystallographic texture could be of advantage. This however will lead to anisotropic first- and second-order bounds, i.e. the effective elastic parameters are governed by directional dependencies, cf. Lobos Fernández and Böhlke (2019).

References

M. Aßmus, R. Glüge, and H. Altenbach. On the analytical estimation for isotropic approximation of elastic properties applied to polycrystalline cubic silicon used at solar cells. *Technische Mechanik*, 40(2):120–133, 2020. doi: 10.24352/ub.ovgu-2020-020.

M. Blackman. On anomalous vibrational spectra. *Proceedings of the Royal Society of London. Series A - Mathematical and Physical Sciences*, 164(916):62–79, 1938. doi: 10.1098/rspa.1938.0005.

P. Ponte Castañeda and P. Suquet. Nonlinear composites. In Erik van der Giessen and Theodore Y. Wu, editors, *Advances in Applied Mechanics*, volume 34, pages 171–302. Elsevier, 1997. doi: 10.1016/S0065-2156(08)70321-1.

P. H. Dederichs and R. Zeller. Elastische Konstanten von Vielkristallen. Technical Report JÜL-877-FF, Kernforschungsanlage Jülich, Institut für Festkörperforschung, Jülich, July 1972. URL http://hdl.handle.net/2128/15202.

G. Dvorak. *Micromechanics of Composite Materials*. Number 186 in Solid Mechanics and Its Applications. Springer, 2013. doi: 10.1007/978-94-007-4101-0.

Z. Hashin and S. Shtrikman. On some variational principles in anisotropic and nonhomogeneous elasticity. *Journal of the Mechanics and Physics of Solids*, 10(4):335–342, 1962a. doi: 10.1016/0022-5096(62)90004-2.

Z. Hashin and S. Shtrikman. A variational approach to the theory of the elastic behaviour of polycrystals. *Journal of the Mechanics and Physics of Solids*, 10(4):343–352, 1962b. doi: 10.1016/0022-5096(62)90005-4.

Z. Hashin and S. Shtrikman. A variational approach to the theory of the elastic behaviour of multiphase materials. *Journal of the Mechanics and Physics of Solids*, 11(2):127–140, 1963. doi: 10.1016/0022-5096(63)90060-7.

R. Hill. The elastic behaviour of a crystalline aggregate. *Proceedings of the Physical Society. Section A*, 65(5):349–354, 1952. doi: 10.1088/0370-1298/65/5/307.

R. Hill. Continuum micro-mechanics of elastoplastic polycrystals. *Journal of the Mechanics and Physics of Solids*, 13(2):89–101, 1965. doi: 10.1016/0022-5096(65)90023-2.

M. A. Hopcroft, W. D. Nix, and T. W. Kenny. What is the Young's Modulus of Silicon? *Journal of Microelectromechanical Systems*, 19(2):229–330, 2010. doi: 10.1109/JMEMS.2009.2039697.

W. F. Hosford. *The Mechanics of Crystals and Textured Polycrystals*. Oxford University Press, 1993.

E. Kröner. *Statistical continuum mechanics*. Number 92 in CISM International Centre for Mechanical Sciences. Springer, 1972. doi: 10.1007/978-3-7091-2862-6.

I. A. Kunin. An algebra of tensor operators and its applications to elasticity. *International Journal of Engineering Science*, 19 (12):1551–1561, 1981. doi: 10.1016/0020-7225(81)90078-1. Dedicated to Prof. K. Kondo on the occassion of his seventieth birthday.

M. Lobos Fernández and T. Böhlke. Representation of Hashin-Shtrikman Bounds in Terms of Texture Coefficients for Arbitrarily Anisotropic Polycrystalline Materials. *Journal of Elasticity*, 134:1–38, 2019. doi: 10.1007/s10659-018-9679-0.

M. A. Michalicek, D. E. Séné, and V. M. Bright. Advanced modeling of micromirror devices. In *Proceedings of the International Conference on Integrated Micro/Nanotechnology for Space Applications*, pages 224–239, Houston, 1995.

G. Milton. *The Theory of Composites*, volume 6 of *Cambridge Monographs on Applied and Computational Mathematics*. Cambridge University Press, Cambridge, UK, 2002. URL http://www.math.utah.edu/books/tcbook.

T. Mura. *Micromechanics of Defects in Solids*. Mechanics of Elastic and Inelastic Solids. Kluwer Academic Publishers, 1987. doi: 10.1007/978-94-009-3489-4.

S. R. Nabavi, F. Haase, E. Jansen, and R. Rolfes. Monte-Carlo simulation of the cofiring process in polycrystalline silicon solar cells: Effects of material heterogeneity and thickness uncertainties. *Solar Energy Materials and Solar Cells*, 170:263–277, 2017. doi: 10.1016/j.solmat.2017.06.012.

J. C. Nadeau and M. Ferrari. On optimal zeroth-order bounds with application to hashin–shtrikman bounds and anisotropy parameters. *International Journal of Solids and Structures*, 38(44):7945–7965, 2001. doi: 10.1016/S0020-7683(00)00393-0.

S. Nemat-Nasser and M. Hori. *Micromechanics: Overall Properties of Heterogeneous Solids*. Elsevier, New York, 1993.

A. Reuss. Berechnung der Fließgrenze von Mischkristallen auf Grund der Plastizitätsbedingung für Einkristalle. *Zeitschrift für Angewandte Mathematik und Mechanik*, 9(1):49–58, 1929. doi: 10.1002/zamm.19290090104.

J. Rychlewski. Unconventional approach to linear elasticity. *Archives of Mechanics*, 47(5):149–171, 1995.

W. N. Sharpe, Bin Yuan, R. Vaidyanathan, and R. L. Edwards. Measurements of Young's modulus, Poisson's ratio, and tensile strength of polysilicon. In *Proceedings IEEE The Tenth Annual International Workshop on Micro Electro Mechanical Systems. An Investigation of Micro Structures, Sensors, Actuators, Machines and Robots*, pages 424–429, 1997.

S. Sutcliffe. Spectral Decomposition of the Elasticity Tensor. *Journal of Applied Mechanics*, 59(4):762–773, 1992. doi: 10.1115/1.2894040.

W. Voigt. *Lehrbuch der Kristallphysik (mit Ausschluss der Kristalloptik)*. Springer, Wiesbaden, 1910. doi: 10.1007/978-3-663-15884-4.

L. J. Walpole. On bounds for the overall elastic moduli of inhomogeneous systems—I. *Journal of the Mechanics and Physics of Solids*, 14(3):151–162, 1966a. doi: 10.1016/0022-5096(66)90035-4.

L. J. Walpole. On bounds for the overall elastic moduli of inhomogeneous systems—II. *Journal of the Mechanics and Physics of Solids*, 14(5):289–301, 1966b. doi: 10.1016/0022-5096(66)90025-1.

J. R. Willis. Bounds and self-consistent estimates for the overall properties of anisotropic composites. *Journal of the Mechanics and Physics of Solids*, 25(3):185–202, 1977. doi: 10.1016/0022-5096(77)90022-9.

J. R. Willis. Variational and related methods for the overall properties of composites. In C.-S. Yih, editor, *Advances in Applied Mechanics*, volume 21, pages 1–78. Elsevier, 1981. doi: 10.1016/S0065-2156(08)70330-2.

R. Zeller and P. H. Dederichs. Elastic constants of polycrystals. *physica status solidi (b)*, 55(2):831–842, 1973. doi: 10.1002/pssb.2220550241.

C. M. Zener. *Elasticity and Anelasticity of Metals*. University of Chicago press, Chicago, 1948.